Evolution of the electronic structure of polyacetylene and polythiophene as a function of doping level and lattice conformation

S. Stafström* and J. L. Brédas†
Laboratoire de Chimie Théorique Appliquée, Facultés Universitaires Notre-Dame de la Paix, rue de Bruxelles 61, B-5000 Namur, Belgium
(Received 22 February 1988)

Band-structure calculations are presented for different lattice conformations of doped polyacetylene and polythiophene. At intermediate doping levels, the intraband transition energies are found to be in good agreement with experimental optical-absorption data for a soliton lattice conformation in polyacetylene and a bipolaron lattice conformation in polythiophene. At high doping levels, where both polymers exhibit a metalliclike behavior, we find the best agreement with observed optical-absorption and magnetic data to occur for a polaron lattice conformation. Important qualitative differences are found between the polaron lattice conformations obtained in this work and those reported previously. The polaron lattice band structures for polyacetylene and polythiophene are calculated to be very similar to one another, which is also consistent with the experimental trends. The evolutions of the π-π^* and the π-to-soliton band energy gaps for polyacetylene are studied and compared with results of the Takayama, Lin-Liu, and Maki (TLM) model. We find that, in comparison with optical data probing these transitions, the valence effective Hamiltonian results are superior to the results of the TLM model. We stress that our results do not constitute a proof of the existence of polaron lattice conformation at high doping levels but indicate that the presence of such a conformation is in agreement with a large number of experimental (ir, optical conductivity, magnetic, electron-energy-loss spectroscopy) data.

I. INTRODUCTION

The discovery a little over a decade ago of high electrical conductivity in doped polyacetylene and subsequently in a large number of doped conjugated polymers has stimulated an enormous amount of work towards the understanding of the electronic and transport properties in conducting organic polymers.[1] It was realized early on that these materials constitute an almost ideal field for the exploration of strong electron-phonon coupling phenomena and many novel and fascinating concepts have been uncovered over the years. For instance, it has been shown that upon doping or photoexcitation, the charges that appear on the polymeric chains are stored in localized defects, which (depending on the kind of polymer or doping level) are solitons, polarons, or bipolarons. The creation of such defects strongly modifies the electronic properties of the polymer, as seen for instance in optical-absorption measurements. These defect species are also thought to be actively involved in the transport properties. However, their exact role in that case is still not fully understood. They appear to act either as charge carriers themselves and/or as sources of electronic states among which conduction electrons can hop; both these processes provide a nonmetallic type of conductivity. Nevertheless, many conducting polymers exhibit a transition into a metallic state at high doping levels. Metallic properties are verified by the finding of high Pauli susceptibility, linear dependence of the thermopower with temperature, and far-ir absorption, i.e., properties which all originate in the appearance of a finite density of states at the Fermi level. However, even in that regime, conducting polymers also appear to have properties not found in normal metals. For instance, the conductivity does not follow the metallic $1/T^2$ law and the persistence of vibrational modes typical of localized defects is in disagreement with the picture of an ordinary metal.

Polyacetylene $[(CH)_x]$ is the first polymer for which a high Pauli susceptibility was found in the highly doped state.[2] Several attempts to explain this phenomenon have been presented. Mele and Rice[3] and Epstein and coworkers[4] showed that band tailing due to disorder and three-dimensional interchain couplings can lead to an incommensurate gapless Peierls system. More recently, Kivelson and Heeger[5] have pointed out that the sharp increase in Pauli susceptibility at about 5% doping could be understood in terms of a first-order phase transition from a soliton lattice to a polaron lattice. Photomodulation spectra of Ehrenfreund *et al.*[6] on doped polyacetylene can be interpreted in this context. However, recent calculations by Choi and Mele[7] have raised doubts about the polaron lattice model since the geometrical structure they find in their calculations is unable to explain the persistence of the doping-induced ir modes.

Following polyacetylene, metalliclike properties were found in poly-*p*-phenylene,[8] polythiophene[9,10] and polypyrrole[9] but only for certain dopant substances; e.g., polypyrrole exhibits a high Pauli susceptibility (χ_P) for BF_4^- dopant[9] whereas there is no sign of χ_P for doping with ClO_4^-.[11] It has also been shown that poly(3-hexylthiophene) in solution exhibits no transition into a metallic state,[12] in contrast to solid-state samples which

become metallic at doping levels $y \sim 0.10$–0.15.[9–10] Recently, polyaniline has also been shown to have metallic properties in its highly conducting (polyemeraldine salt) state.[13] Arguments based on an internal reduction-oxidation reaction[13,14] into a polaron lattice were used to explain the metallic properties. A theoretical study of the polaron lattice in fully protonated polyemeraldine, based on the same tools as in this work, has provided excellent agreement with experimental results.[15]

In this study, we report on geometry, charge density, and electronic band-structure calculations on *trans*-polyacetylene and polythiophene. Our goals are (i) to describe band-structure evolution as a function of the concentration in different defects, i.e., as a function of doping level assuming solitons, bipolarons, or polarons to be stable; and (ii) to examine the so-obtained band structures in the light of available experimental data. We start by introducing the methodology in Sec. II. The geometry and charge distribution associated with the defects are discussed in Sec. III. In Sec. IV we present the electronic properties of *trans*-polyacetylene and polythiophene in the low and intermediate doping regimes. Finally and most extensively, in Sec. V, we discuss the electronic properties of the highly doped polymers, i.e., in the regime where the defects interact strongly and a metallic state is experimentally found.

II. METHODOLOGY

Because of the large electron-phonon coupling present in conjugated polymeric systems, care has to be taken of geometrical relaxation effects along the polymer chains upon doping. Different methods, ranging from the relatively simple Su-Schrieffer-Heeger (SSH) Hückel-like Hamiltonian[16] to sophisticated *ab initio* techniques[17,18] have been used to calculate the geometries of doped systems, as well as those of pristine chains. We have chosen to use the semiempirical MNDO (modified neglect of diatomic overlap) method of Dewar and Thiel.[19] In an earlier work by Boudreaux *et al.*,[20] this method was successfully used to calculate geometries and charge distributions associated with isolated solitons and polarons in *trans*-$(CH)_x$. Our results on this polymer are in full agreement with what these authors have obtained and will therefore be discussed only briefly here. For polythiophene, we perform geometry optimizations on oligomers containing up to six thiophene units. We note that doped thiophene tetramers have already been studied theoretically using the *ab initio* Hartree-Fock STO-3G method.[17] We believe, however, that for the purpose of our work, the tetramer is too small a system to give a full picture of the complete defect geometry. Furthermore, it has also been recognized that the use of a minimal basis set exaggerates the degree of bond-length alternation along the carbon backbone of the polymer. For instance, using an STO-3G basis set, the bond-length alternation in polyacetylene is calculated to be 60% larger than the result obtained by using a double-ζ basis set, which in turn is very similar to the MNDO result (see below). We stress that one advantage of the MNDO method as compared to Hückel-type techniques is that it is self-consistent and therefore provides information about charge distributions with reasonable accuracy. This is an important feature in order to understand the transport properties of the material.

On the basis of MNDO-optimized geometries, the electronic structures of *trans*-polyacetylene [*trans*-$(CH)_x$] and polythiophene (PT) are studied in a stereoregular conformation with the nonempirical valence effective hamiltonian (VEH) pseudopotential method. This technique has been developed for molecules by Nicolas and Durand[21] and extended to polymers by André *et al.*[22] VEH band-structure calculations have been performed on a number of conjugated polymers (e.g., polyacetylene,[23] polyparaphenylene,[17] polythiophene,[17] polypyrrole,[17] and recently polyaniline[15]) including doping-induced geometry relaxations. The suitability of the VEH technique for describing the electronic structure of these compounds is illustrated by the excellent agreement between the photoemission (x-ray or ultraviolet photoemission spectroscopy) valence-band spectra and the VEH-calculated spectra.[24] It is also our experience that the VEH band structures provide good estimates for the energies of the first optical transitions and are well suited for the studies of the transitions involving the defect bands.

Briefly described, the calculation procedure is the following. Geometry optimizations in the presence of defects are performed on the following oligomers: (i) $[H\text{-}(CH)_{40}\text{-}H]^{+\bullet}$ for the polaron and $[H\text{-}(CH)_{41}\text{-}H]^{+}$ for the soliton in *trans*-$(CH)_x$; (ii) $[H\text{-}(SC_4H_2)_6\text{-}H]^{+\bullet}$ for the polaron and $[H\text{-}(SC_4H_2)_6\text{-}H]^{2+}$ for the bipolaron in PT. The size of these oligomeric systems is chosen to be big enough as to avoid major influences of end effects in the optimized geometry of the defects. To reduce the number of variables in the optimization problem, we impose a central symmetric configuration to each oligomer; furthermore, all C—H bond lengths are held at 1.09 Å. Except for these restrictions, we allow for a full geometry relaxation of the system.

The geometry obtained from the MNDO optimization of the cation or dication oligomers is then used to define the unit-cell conformation for VEH band-structure calculations. Each unit cell is chosen to contain a single defect. In this way, the size of the unit cell determines the doping level of the polymer chain. The unit cells and the corresponding doping levels (y) treated in this study are the following: (i) for *trans*-$(CH)_x$, we have considered three soliton unit cells, $(CH)_{29}^{+}$ ($y=0.034$), $(CH)_{23}^{+}$ ($y=0.043$), and $(CH)_{17}^{+}$ ($y=0.058$) and one polaron unit cell of size $(CH)_{16}^{+\bullet}$ ($y=0.0625$); (ii) for PT, we have considered three bipolaron unit cells, $(C_4H_2S)_{10}^{2+}$ ($y=0.20$), $(C_4H_2S)_8^{2+}$ ($y=0.25$), and $(C_4H_2S)_6^{2+}$ ($y=0.33$) and three polaron unit cells, $(C_4H_2S)_{10}^{+\bullet}$ ($y=0.10$), $(C_4H_2S)_4^{+\bullet}$ ($y=0.25$), and $(C_4H_2S)_3^{+\bullet}$ ($y=0.33$). Note that, for example, in the polaron unit cells of *trans*-$(CH)_x$ at doping level $y=0.0625$ and PT at doping level $y=0.25$, there is exactly the same number of carbon atoms per unit charge, even though the doping levels as indicated by y are quite different. We also point out that the minimal unit cell in a soliton lattice calculation contains an odd number of CH units while both bipolaron and polaron cells contain an even number of CH

units.

The approach of using the geometry optimized on finite systems in calculations for infinite systems has been questioned in the literature. Using the continuum model of Takayama, Lin-Liu, and Maki (TLM),[25] Choi and Mele[7] found that the bond-length alternation for the polaron lattice configuration of an infinite *trans*-$(CH)_x$ chain does not closely resemble that constructed from a superposition of isolated polarons. The lattice polaron they found is considerably more delocalized and possesses a very small deviation from the perfect bond-length alternation pattern at the defect center. Choi and Mele also found that above $y=0.06$, the polaron lattice is even unstable with respect to an undimerized conformation. We will come back to these points later.

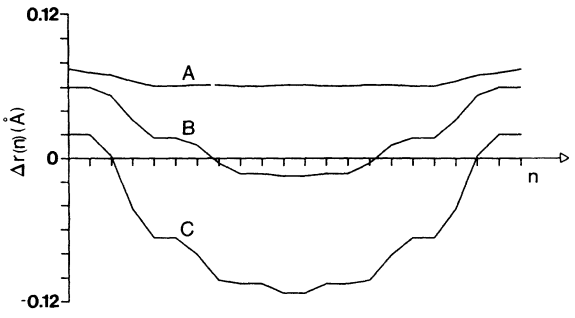

FIG. 1. Bond-length alternation pattern, Δr, in Å for the C—C bonds, n, along the hexathiophene oligomer. Curve *A*, neutral system; curve *B*, singly charged system (polaron); and curve *C*, doubly charged system (bipolaron).

III. GEOMETRY AND CHARGE DISTRIBUTION

The optimized bond lengths at the center of the neutral polyacetylene chain are 1.463 and 1.357 Å for the single and double bonds, respectively. This gives a degree of bond-length alternation $\Delta r_0=0.106$ Å, in good agreement with experimental estimates $\Delta r_0 \sim 0.08-0.10$ Å.[26] *Ab initio* double-ζ calculations by Karpfen and Petkov[27] and Villar and Dupuis[18] give shorter bond lengths than with the MNDO method (Ref. 27: C=C, 1.346 Å and C—C, 1.446 Å; Ref. 18: C=C, 1.338 Å and C—C; 1.450 Å) but very similar bond-length alternation (Ref. 27: $\Delta r_0=0.100$ Å and Ref. 18: $\Delta r_0=0.112$ Å).

The positively charged soliton exhibits a smooth change in the bond-length alternation pattern from the so-called *A* phase (double-bond–single-bond alternation) to the *B* phase (single-bond–double-bond alternation). The evolution fits nicely into a $\tanh(n/\xi)$ function for $\xi=5$ (where ξ is the soliton coherence length and n the site position away from the defect center). Compared to the SSH result (which is best fitted by $\xi=7$),[16] MNDO leads to a slightly more localized soliton. For the positive polaron, there occurs a partial depression of the bond-length alternation which reaches a minimum of $\Delta r=0.49\Delta r_0$ in the middle of the defect. In contrast to the soliton case, the MNDO result yields a more extended polaron than what is found by the SSH model.

The bond-length alternation patterns of the neutral, singly, and doubly charged thiophene hexamers are displayed in Fig. 1. The singly and doubly charged systems should be regarded as polaron and bipolaron units, respectively. In the neutral oligomer, we find the innermost rings to have the following bond lengths: S—C_α is 1.701 Å, C_β—C_β is 1.443 Å, C_α—C_β is 1.383 Å, and the inter-ring C_α—C_α bond is 1.444 Å. The maximum change in any of these bond lengths along the chain is less than 0.01 Å, which shows that the end effects are in this case very small. We note from Fig. 1 that the neutral system has an almost perfect bond-length alternation along the *cis-trans* carbon backbone with an alternation degree $\Delta r=0.06$ Å, i.e., considerably smaller than the corresponding value in *trans*-$(CH)_x$. This is qualitatively consistent with the aromatic nature of the thiophene ring. A comparison can be made with *ab initio* STO-3G calculations on quaterthiophene giving the following optimized bond lengths: S—C_α is 1.721 Å, C_β—C_β is 1.444 Å, C_α—C_β is 1.346 Å, and the inter-ring bond is 1.480 Å.[17] There is a rather large difference between the MNDO and STO-3G results as concerns the degree of bond-length alternation along the carbon backbone of the system. As noted in the preceding section, this discrepancy is to some extent accounted for by the tendency of the STO-3G method to exaggerate the degree of bond alternation. We will return to a discussion of the impact of this difference on the electronic properties of the material later in this section. No precise crystallographic data have been reported on PT. The only closely related structure that has been determined is that of gaseous bithiophene,[28] where geometrical constants close to the *ab initio* results are found. This molecule is, however, believed to be significantly twisted, which makes the comparison less relevant.

The geometry of the positive polaron unit, presented in Fig. 1, exhibits almost identical carbon-carbon bond lengths (i.e., $\Delta r \sim 0$ Å) in the center (see Fig. 1). The maximum change of the bond lengths, as compared to the neutral case, is 0.04 Å. A smooth evolution of the geometry to approach that of the neutral system is found when moving away from the center of the oligomer. The geometry of the rings at the ends of the hexamer is identical to that of the neutral system. This indicates that the structural width of the polaron is ~4 rings, a value in very good agreement with Hückel SSH-type estimates of the delocalization of the spin associated with the polaron defect.[29] The S—C_α distance is almost constant over the whole polaron suggesting a very small contribution from the sulfur atom to the polaron state. This finding is confirmed by inspection of the polaron wave function at the MNDO level. The lack of sulfur contribution to the occupied polaron state suggests similar geometric and electronic structures for the polarons in PT and in *trans*-$(CH)_x$. This similarity holds as far as geometrical extension and evolution of the bond-length alternation (in both cases, decrease by about 0.06 Å) of the defect are concerned. The difference lies in the almost complete removal of the bond-length alternation at the center of the polaron in PT, whereas in *trans*-$(CH)_x$ the alternation still persists to about 50% at the defect center. Given the

similarities in the evolution of the bond-length order parameters this discrepancy is mostly due to the different ground-state bond alternations of the two polymers (see above).

The geometry of the bipolaron unit shows a quinoid-like structure at the center, i.e., an interchange of the single and double bonds as compared to the undoped case (see Fig. 1). The bipolaron is clearly wider than the polaron. In our six-ring system, the end rings have bond lengths which differ by 0.02 Å from those of the neutral system and possess a geometrical structure similar to that of the rings which mark the end of the polaron defect (i.e., rings 2 and 5 of the singly charged unit). We assume, therefore, that in the doubly charged unit, rings 1 and 6 play about the same role and also mark the end of the bipolaron defect. This gives an extension of the bipolaron that exceeds that of the polaron by at least 50%. The larger extent of the bipolaron is easily understood in terms of the stronger Coulomb repulsion present in the doubly charged unit, which acts to separate the charges as much as possible. In nondegenerate ground-state polymers, such as polythiophene, this repulsion is balanced by the increase in energy due to the appearance of more energetically unfavorable quinoid units, leading to bipolaron formation. Brédas *et al.*[29] and Bertho and Jouanin[30] have studied the geometrical and electronic properties of bipolarons and polarons in PT using an SSH-type Hamiltonian. In contrast to what is found using the MNDO method, they find an equal geometrical extension for the two defects. This discrepancy is most probably due to the fact that no electron-electron interaction terms are explicitly included in the SSH model, which tends to reduce the effects of charge separation as discussed above.

The change in S—C_α bond lengths relative to the neutral oligomer is 0.01 Å at the bipolaron center, compared to 0.001 Å for the polaron unit. This larger change can be traced back to the different occupation of the p_z orbital of the sulfur atom at the center of the defects and will be discussed in more detail below.

In Fig. 2 we show the excess charges for the singly (polaron) and doubly charged (bipolaron) systems relative to the neutral hexathiophene oligomer. A similar diagram for the net charges of soliton and polaron in *trans*-$(CH)_x$ is found in Ref. 20. As seen from Fig. 2, the effect of the added charge(s) is to set up a charge density wave (CDW) along the carbon backbone of the polymer chain. The CDW is clearly more delocalized than the geometrical defect itself. Except for a factor of roughly 2 in the values of the charges, the CDW is very similar in the singly and doubly charged thiophene systems. We find the largest amplitude of the oscillations to be located about two rings away from the center and the largest absolute values of the charges to be mostly present on the C_α carbons. There is a strong similarity between CDW in PT and that in *trans*-$(CH)_x$. The appearance of such a CDW is not surprising, it is predicted even with simple Hückel theory. It should be noted that MNDO yields charge oscillation values larger than those found in *ab initio* double-ζ calculations on the positively charged soliton in *trans*-$(CH)_x$. The *ab initio* results indicate maximum net charges of $+0.18$ and -0.04,[18] to be compared to MNDO values of $+0.26$ and -0.13. The sums of those charges are, however, calculated to be almost identical with both approaches: $+0.14$ and $+0.13$ at the *ab initio* and MNDO levels, respectively.

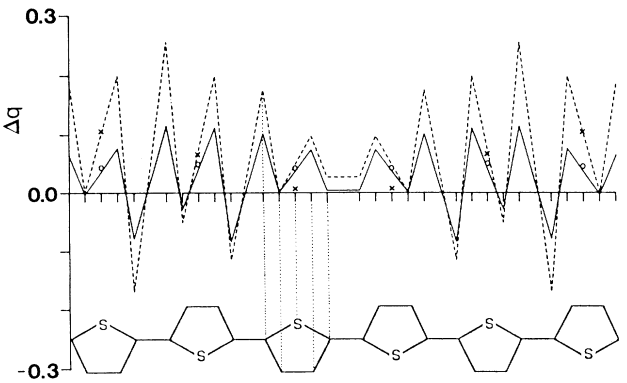

FIG. 2. Excess atomic charges, Δq (in $|e|$), for the singly charged (polaron) (solid line, sulfur: open circles) and doubly charged (bipolaron) (dashed line, sulfur: crosses) thiophene hexamers relative to the neutral system. The positions of the atoms are indicated by the sketch of the oligomeric system given directly below the diagram. The lines between the site positions are drawn to guide the eye.

A remarkable change in the charge density on the sulfur atoms in the central part of the oligomer is observed when going from the singly charged to the doubly charged system. We find that by removing the second electron from the system, these central sulfur atoms become less positively charged (see Fig. 2). This increase in electron charge density is entirely due to an increase in the population of the p_z atomic orbitals and is a result of an enhancement of the on-site Coulomb repulsion on the central atoms compared to the outer sites.[31]

IV. NONINTERACTING DEFECTS

A. Polyacetylene

To be able to study the evolution of the effects of doping on the electronic structure, we have first computed the VEH band structure of undoped *trans*-$(CH)_x$. Part of the π-band structure is shown in Fig. 3 (dotted line). With the geometry from the MNDO optimization, the Peierls gap, i.e., the energy gap between the occupied and unoccupied states, is calculated to be 1.43 eV and the total π-band width is 13.6 eV. The band gap agrees very well with experimentally observed frequency-dependent conductivity data on *trans*-$(CH)_x$, which exhibit a maximum at 1.4 eV interpreted as due to the π-π^* transition.[32] Slightly different results are found from optical-absorption data, which onset at ~ 1.4 eV and peak at ~ 1.8–1.9 eV.[33]

To determine the electronic properties at low and intermediate doping levels, we have performed a VEH band-structure calculation for *trans*-$(CH)_x$ in the soliton lattice conformation. The distance between two solitons

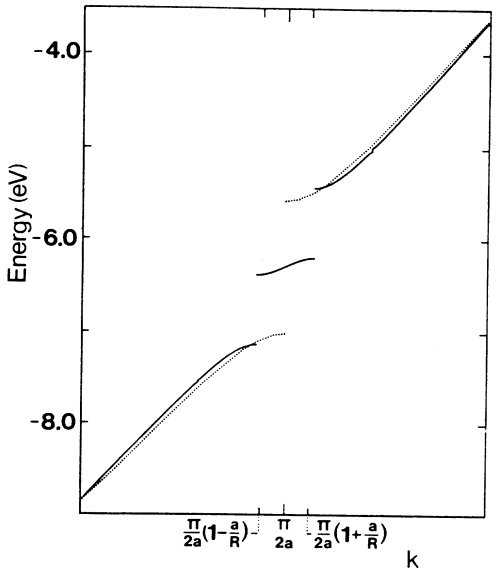

FIG. 3. VEH band structure for the perfectly dimerized (dotted lines) and soliton lattice (solid lines) conformations of *trans*-polyacetylene. The distance between neighboring solitons, R, is 29 CH units, corresponding to a doping level of $y=0.034$.

is chosen in this case to be 29 CH units and defines the unit cell of the polymer. This choice of unit cell corresponds to a doping level $y=\frac{1}{29}=0.034$. The band structure in the extended zone scheme presentation is displayed in Fig. 3 together with the band structure of the undoped polymer. The midgap soliton band is 0.16 eV wide; the subgaps appearing on both sides of the soliton band are almost equivalent (about 0.75 eV), which means that the electron-hole symmetry is rather well preserved at the VEH level of calculation.

Except near the Peierls gap, the two band structures are practically indistinguishable. No additional gaps can be detected at multiples of π/R (where R corresponds to the lattice constant), which is due to the fact that opening of gaps inside the occupied band does not lead to any lowering of the electronic energy. The value of the energy gap between the valence band and the unoccupied soliton band (0.75 eV) compares favorably with the experimentally observed doping-induced optical-absorption,[33] and frequency-dependent conductivity results,[32] which both peak at 0.7 eV. Furthermore, we calculate the π-π^* transition to onset at 1.68 eV. Again, we find very good agreement with the experimentally observed value of 1.6 eV obtained from the optical conductivity studies.[32]

Jeyadev and Conwell[34] pointed out that, in the framework of the TLM model,[25] the oscillator strength vanishes for a π-π^* interband transition involving valence- and conduction-band states located in a perfectly symmetric way relative to the Fermi energy of the undoped polymer. We note that the VEH calculations do not predict a perfectly symmetric evolution of these states. Therefore, the interband transition has to not be totally suppressed.

B. Polythiophene

At the VEH level, undoped polythiophene presents a gap between the highest occupied and lowest unoccupied bands of 1.7 eV on the basis of the MNDO-optimized geometry. We can compare this value with that obtained from a VEH calculation using the STO-3G geometry. Since the STO-3G-optimized geometry shows a stronger bond-length alternation along the carbon backbone of the chain, the band gap is found to be larger, 2.2 eV.[17] These theoretical values should be compared with the onset energy of the optical absorption, which is found at 2.0 eV.[35] This suggests that the effective degree of bond alternation in the polymer is somewhere between that of the STO-3G- and MNDO-optimized geometries (i.e., somewhat underestimated in the MNDO case and overestimated in the STO-3G case).

It has been observed that in some cases [e.g., BF_4^- doped PT (Ref. 36) and electrochemically doped poly(3-methylthiophene)],[37] light doping of PT (in the solid state) results in an increase of the spin density of the polymer. The increase in the number of spins is comparable to the number of injected charges, which suggests that these charges are stored as polarons.[36,37] The optical-absorption spectrum of the lightly doped samples exhibits a rather sharp peak at 1.3 eV, interpreted as a transition between the two polaron gap states. Both the spin density and this absorption peak disappear at doping levels above $y=0.05$, suggesting a recombination of the polarons into bipolarons.[36] (Note that in other cases, e.g., ClO_4^- electrochemical doping of PT films, no evidence for polarons is found even for doping levels as small as $y=0.0235$.) A fruitful comparison can be made with our calculation on the low-density polaron lattice. The band structure of this system is presented in Fig. 4(a). Even though the doping level is quite high, $y=0.10$, the polaron bands are very narrow [widths of only 0.11 and 0.08 eV for the lower (band b) and upper (band c) polaron bands, respectively], indicating a very small interaction between the polarons. It is therefore expected that the transitions involving these polaron bands constitute a good approximation to those in the limit of zero bandwidth. The value for the transition between the polaron bands b and c is calculated to be $\omega_2=1.41$ eV, i.e., in close agreement with the absorption observed at 1.3 eV. Furthermore, in the data of Kaneto *et al.*,[36] additional weak absorptions in the lightly doped samples are seen at ~ 0.5 and 1.9 eV. Corresponding interband transitions [see Fig. 4(a)] are calculated to onset at $\omega_1=0.32$ eV (between bands a and b) and $\omega_3=1.73$ eV (between bands a and c).

We must, however, be somewhat cautious when comparing the calculated transition energies with the experimental data. Even though we have seen that, for $y=0.10$, the defects regularly placed along the polymer chain hardly overlap with each other, there occurs a large deformation of the lattice relative to the undoped polymer since the structural defects extend over 4–6 thiophene rings (see Sec. III) and we are dealing with strongly electron-phonon coupled systems. Moreover, since the polaron concentration is rather high in the cal-

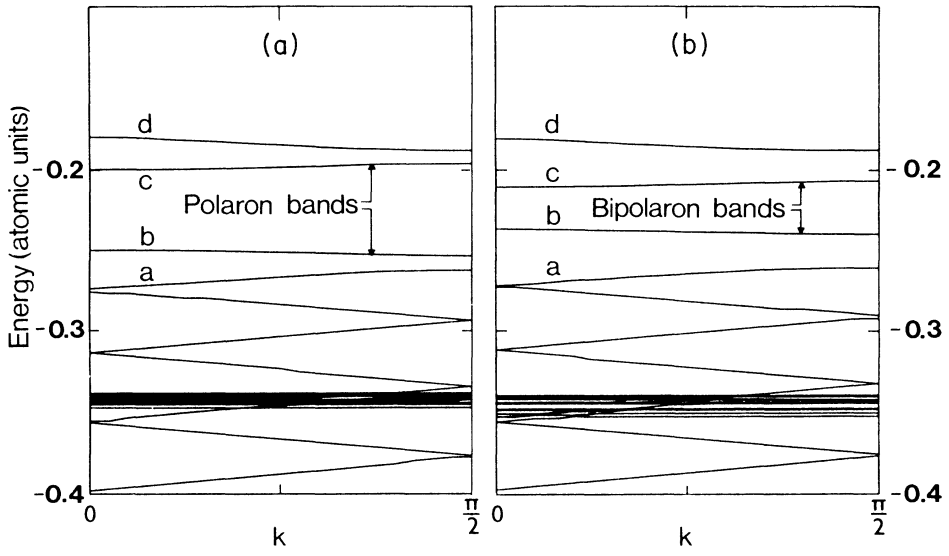

FIG. 4. VEH band structure for polythiophene: (a) the polaron lattice at doping level $y=0.10$ and (b) the bipolaron lattice at doping level $y=0.20$.

culations, there are more states removed from the valence and conduction bands in the theoretical band structure than would be the case for the lightest doping levels experimentally achievable. As a result, some discrepancies between the theoretical and experimental data should be expected for the positions of the valence- and conduction-band edges. For example, we find the energy of the π-π^* transition to increase by 0.30 eV for the smallest doping level considered theoretically ($y=0.10$) compared to the undoped case. Such a large change does not occur experimentally when the doping level is around $y=0.01$. The fact that ω_1 and ω_3 involve transitions from the valence band thus indicates that estimates of these transition energies are less precise than for the transition *between* the polaron bands. It is interesting to note that the difference between the experimental absorption peaks at 0.5 and 1.9 eV is 1.4 eV, i.e., in almost perfect agreement with what we calculate, namely, $\omega_1-\omega_3=\omega_2=1.41$ eV. Note that by comparing these difference values we not only eliminate the errors in the valence- or conduction-band edges for the theoretical spectra, but also the influence of the Coulomb attraction between the dopant ions and the defects on the experimentally observed transitions.

The isolated polaron in polythiophene was recently studied by Bertho and Jouanin[30] and Brédas *et al.*[29] using an SSH-type Hamiltonian with parameters optimized to fit experimental data for neutral polythiophene. For the hole polaron, the following energies of the ω_1, ω_2, and ω_3 transitions were found: 0.4, 1.35, and 1.75 eV (Ref. 30) and 0.34, 1.43, and 1.77 eV (Ref. 29). These values are all in very close agreement with our results as well as the experimental results.

Since the bipolaron is doubly charged, the unit cell is twice as large as in the polaron case for a given doping level; e.g., to represent the bipolaron lattice at $y=0.05$, we need a unit cell of 40 thiophene rings containing 960 valence electrons. This would clearly be an intractable problem to solve. However, from the geometry optimization, we have seen that the structural width of the bipolaron is roughly six monomers. Assuming that the tails of the electronic state associated with the bipolaron extend somewhat outside this region, we expect the onset of bipolaron-bipolaron overlap to occur at roughly $y=0.20$, i.e., one bipolaron per ten thiophene units. The band structure for this doping level is shown in Fig. 4(b). The bipolaron bandwidths are 0.11 and 0.08 eV for the lower and upper bipolaron bands, respectively. These results show that $y=0.20$ is indeed almost within the noninteracting regime and significant comparisons can be made with experimental data reported for lower doping levels. In this context, it is worthwhile to point out again that our theoretical studies are performed on perfectly regular lattices whereas, experimentally, there can exist a more or less random structural distribution of the doping-induced defects. The optical-absorption spectra naturally show some signature of this randomness as well as other perturbing effects not present in our calculations. This makes a direct translation of our ideal y value for the one-dimensional lattice into the experimental doping level difficult and only qualitative agreement is expected.

For the VEH band structure for the bipolaron lattice at doping level $y=0.20$, shown in Fig. 4(b), we find transitions from the valence band (band *a*) to the bipolaron bands (bands *b* and *c*) to occur at energies $\omega_1=0.57$ eV and $\omega_2=1.47$ eV, respectively. These values are in good agreement with the experimentally observed absorptions at ~ 0.65 and ~ 1.5 eV for PT doped within the range $0.05<y<0.10$.[35] The VEH result is also in agreement with results obtained using an SSH Hamiltonian.[29,30] Bertho and Jouanin[30] find the ω_1 and ω_2 transitions at 0.7 and 1.4 eV and Brédas *et al.*[29] locate them at 0.50 and 1.60 eV, respectively.

The large electron-phonon coupling present in conju-

gated polymer systems also leads to formation of localized defects following photoexcitation, i.e., an electron-hole pair in the rigid band picture is unstable with respect to the creation of defects such as solitons, polarons, or bipolarons. The photoinduced absorption spectrum for PT shows two symmetric absorptions peaking at 0.45 and 1.25 eV.[38] These peaks are attributed to the ω_1 and ω_2 transitions involving bipolaron states, since no spins are observed to be created in the photoexcitation process. In comparison with the corresponding values for doping-induced bipolarons, a shift of about 0.2 eV is observed for the two peaks. This shift is an effect of the Coulomb interaction between the dopant ion and the bipolaron, which is present only in the case of doping-induced defects. As noted above, it is more appropriate to study the difference between the two absorption energies due to bipolarons. It is an important feature of our results that this difference is observed to be almost identical in the three cases, namely, $\omega_1-\omega_2=0.90$ eV in our theoretical spectra and 0.85 eV for both photo- and doping-induced bipolarons. The SSH-type calculations of Brédas *et al.*[29] lead to slightly larger separation of the bipolaron states, $\omega_1-\omega_2=1.1$ eV. This is expected since, as noted above, the geometrical distortion associated with the bipolaron is shallower at the Hückel level, which produces bipolaron states closer to the band edges. The results of Bertho and Jouanin[30] ($\omega_1-\omega_2=0.70$ eV) are in this context more difficult to understand.

To conclude this section, we point out that the VEH band structures for dilute polaron concentration (in PT) and for moderate soliton [in *trans*-$(CH)_x$] or bipolaron (in PT) concentrations lead to very good agreement between experimental and theoretical optical transitions. Thus, our results support the interpretation of the absorption data at light doping in terms of a soliton model in *trans*-$(CH)_x$ and of polarons, recombining into bipolarons at intermediate doping levels in BF_4^- doped polythiophene.

V. INTERACTING DEFECTS

Discussion now focuses on the band structures obtained in the highly doped regime, i.e., when solitons, bipolarons, or polarons strongly interact. As discussed in the Introduction, this regime is of special interest because it exhibits metallic properties. The results for *trans*-polyacetylene and polythiophene are first presented separately and then discussed and compared together.

A. Polyacetylene

As an introduction to the study of interacting defects, it is of interest to present a comparison between our results for the soliton lattice and the results obtained from the lattice version of the continuum TLM model.[25] Within this model, Horowitz[39] has derived analytic expressions for the energy of the band edges in the soliton lattice. With the zero-energy reference located at the soliton band center, he found the valence- and conduction-band edges at energies $-\Delta_1/q$ and $+\Delta_1/q$, respectively, and the soliton band extending between $-\Delta_1 q'/q$ and $+\Delta_1 q'/q$. Here, Δ_1 is the amplitude of the lattice order parameter $\Delta(x)$ to be determined self-consistently.[39] The variables q and q' depend on the doping level and have to be derived from the following self-consistent equations:

$$q(y)=(2\xi)^{-1}[yK(q)]^{-1} \tag{1}$$

and

$$q'(y)=\{1-[q(y)]^2\}^{-1/2}\ , \tag{2}$$

where ξ is the soliton coherence length, y the doping level, and $K(q)$ the complete elliptic integral. Following the derivation of Horowitz, the following expressions are obtained for the changes in the valence- to conduction-band gap ($\Delta E_{\pi-\pi^*}$) and the valence- to soliton-band gap ($E_{\pi-s}$):

$$\Delta E_{\pi-\pi^*}/E_0=\Delta_1[(q-1)\Delta_0] \tag{3}$$

and

$$E_{\pi-s}/E_0=(\Delta_1/\Delta_0)[(1-q')/q]\ , \tag{4}$$

where E_0 is the valence- to conduction-band gap for the perfectly dimerized chain. We have used the SSH values of the parameters appearing in the equations, resulting in a soliton coherence length, $2\xi=14$. The solutions of Eqs. (3) and (4) are shown in Figs. 5(a) and 5(b), respectively, together with the corresponding VEH results for doping levels $y=0.034$, $y=0.045$, and $y=0.058$. We observe that, for the range of doping levels examined here, the VEH method gives a nearly linear evolution of the energy gaps as a function of doping level. In particular, there is a very large deviation between the two methods as concerns the soliton bandwidth. For instance, at $y=0.045$ the VEH result is 0.36 eV compared to 1.18 eV found by solving the equations above. The result is only partially due to the shorter soliton coherence length that is optimized by the MNDO method, $2\xi=10$, and used in the VEH calculation. With this smaller value for the coherence length, a soliton-band width of 0.68 eV is found from Eqs. (3) and (4), i.e., a value almost twice as large as the VEH result. This shows that the VEH method, as such, gives a narrower soliton band.

In Figs. 5(a) and 5(b), we also include experimental results from a study of the frequency-dependent conductivity.[32] The energies for the π-π^* transition and the valence- to soliton-band transition are taken from the peak values of the spectra presented in Fig. 2 of Ref. 32. The band gap of the undoped polymer (E_0) is in this study 1.4 eV, i.e., close to the values found by both VEH and TLM methods. The evolution of the experimental data is in much better agreement with the VEH results than what is found by the TLM method and thus supports the validity of the VEH approach for these systems. It deserves to be stressed that no signature of the π-π^* transition is observed experimentally for the sample doped to $y=0.061$, in contradiction to the VEH result for the *soliton lattice* at corresponding doping level, suggesting that at such doping levels, a soliton lattice conformation is no longer present.

The VEH band structure of highly doped *trans*-$(CH)_x$

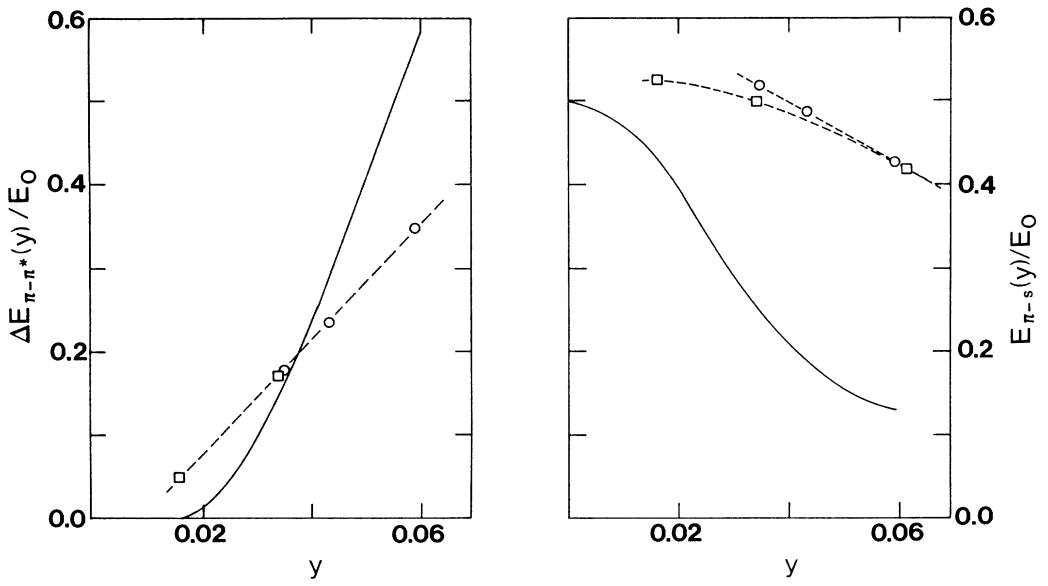

FIG. 5. Evolution, as a function of doping level y, of (a) the normalized gap between the valence and conduction bands ($\Delta E_{\pi-\pi^*}/E_0$) and (b) the normalized gap between the valence and soliton bands ($E_{\pi-s}/E_0$) for *trans*-polyacetylene. The solid lines represent the solution of Eqs. (3) and (4), the circles are the results of VEH calculations, and the squares indicate the experimental values obtained from Ref. 32.

is presented in Fig. 6(a) for the soliton lattice conformation ($y=0.058$) and in Fig. 6(b) for the polaron lattice conformation ($y=0.0625$). Note that the reciprocal unit cell of the polaron lattice is about 6% larger than the one of the soliton lattice. The soliton band [band c in Fig. 6(a)] is 0.74 eV wide and the subgaps appearing on both sides of this band are 0.62 and 0.60 eV for the lower and upper gaps, respectively. In the polaron band structure, there appear two bands within the Peierls gap, bands b and c in Fig. 6(b). The widths of the lower and upper polaron bands are 0.95 and 0.94 eV, respectively. The two polaron bands are separated (at $k=0$) by 0.85 eV and are 0.09 eV away (at $k=\pi/R$) from the conduction- or valence-band edges. It is notable that the VEH method gives polaron bands that are *wider* than the soliton band. The appearance of highly dispersive bands in the metallic regime is also experimentally verified from electron-energy-loss-spectroscopy (EELS) studies on doped highly oriented *trans*-$(CH)_x$.[40] In earlier, more qualitative theoretical studies, the polaron bands have been presented as rather narrow, essentially dispersionless, bands.[5] The disagreement between this latter result and the EELS experimental findings has been used as an argument against the polaron lattice model. It is therefore important to point out that the VEH results for the polaron lattice are in perfect qualitative agreement with the EELS data.

When comparing Figs. 6(a) and 6(b), an interesting feature is that the half-filled polaron band neatly fits into the gap (between the valence band and the soliton band) at the Fermi level of the soliton lattice. Therefore, excitations across this gap in the soliton lattice become comparable in energy to *intraband* excitations in the half-filled polaron band. This feature has important consequences for the comparison with experimental optical-absorption data.

The first interband transition in the soliton lattice [between bands b and c of Fig. 6(a)] is calculated to onset at 0.62 eV. In the polaron lattice, we must take into account the intraband transition within the half-filled polaron band [band b in Fig. 6(b)]. Optical absorption within this band is expected in the far ir up to an energy roughly corresponding to the width of the polaron band, i.e., ~ 1.0 eV. We may recall that optical transitions are strictly allowed only if k vector (momentum) can be conserved. However, we can expect some disorder effects to be present, which will destroy the symmetry of the lattice and thus the importance of the k-conservation rule.

Another important aspect of our results is the large difference in the π-π^* energy gap. Taking into account the proper unit cell for the soliton lattice, we obtain a direct band gap of 2.0 eV, compared to 2.9 eV for the polaron lattice. This difference is most easily understood by the fact that there are twice as many bands in the band gap for the polaron lattice since each polaron brings two states into the gap while each soliton only brings one state into the gap. It must be stressed, however, that no oscillator strengths are considered in our model, which can make the comparison with experimental data more difficult in some instances.

Optical conductivity data on doped *trans*-polyacetylene (including the low-frequency region)[32] show that above the critical doping concentration at which the polymer enters a metalliclike regime there occurs a rounding of all optical transitions in the 0.5–2.5-eV region and a marked increase of absorption in the far ir. The first absorption peak shifts slightly down to 0.6 eV and the absorption previously related to the π-π^* transition is no longer observed.

Clearly, above 5–6% doping, the soliton lattice con-

formation fails to explain the optical data in the far-ir region (since the excitation gap would be 0.6 eV in this case) as well as the magnetic data. Instead, the far-ir absorption could be well understood as originating from intraband absorption within the half-filled polaron band in the polaron lattice. The softening of the π-π^* transition is in agreement with our calculations showing that in the polaron lattice the π-π^* transition shifts to ~ 2.9 eV. Furthermore, for the polaron lattice, besides intraband excitations, optical transitions at 1.3 eV (from band *a* to band *b*), 1.6 eV (from band *b* to band *c*), and 2.8 eV (from band *b* to band *d*) are also predicted. This is in qualitative agreement with the rounding of the absorption data between 0.5 and 2.5 eV. Disorder effects can also lead to further rounding of these absorptions since around the doping levels where the metallic transition takes place, the widths of the polaron (or soliton) bands are very dependent on the actual doping levels. Indeed, the widths of the defect wave functions being of the order of 15–20 sites, slight local modifications in the actual doping level can significantly change the overlap between defect wave functions.

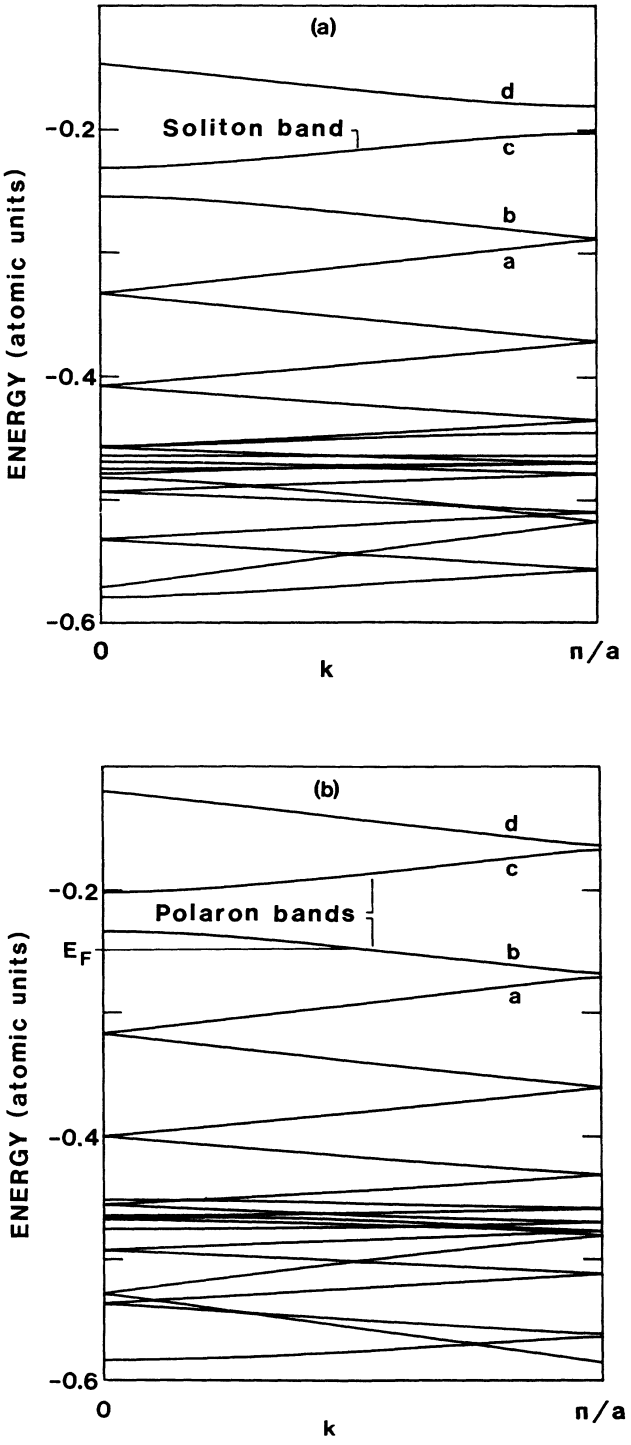

FIG. 6. VEH band structures for *trans*-polyacetylene: (a) the soliton lattice at doping level $y=0.058$ and (b) the polaron lattice at $y=0.0625$.

B. Polythiophene

The band structure of polythiophene in the bipolaron and polaron lattice conformations for $y=0.25$ are shown in Figs. 7(a) and 7(b), respectively. Note that the length of the reciprocal unit cell in the bipolaron lattice is about half the one of the polaron lattice and contains twice as many bands. A comparison of the main features of the band structures for the two lattice conformations calls for the following remarks.

(i) Conceptually, if we go from the polaron lattice [Fig. 7(b)] to the bipolaron lattice [Fig. 7(a)], the two polaron bands [*b* and *c* in Fig. 7(b)] are split into four bands [*b*, *b'*, *c*, and *c'* in Fig. 7(a)], the middle two (bands *b'* and *c*) residing in the gap as bipolaron bands; it is therefore apparent that the π-π^* gap (between bands *b* and *c'*) in the bipolaron lattice is smaller than that (between bands *a* and *d*) in the polaron lattice.

(ii) The Fermi level (or chemical potential) appears at about the same energy in both cases.

(iii) The bipolaron bands lie deeper into the intrinsic band gap.

These differences in the band structure between the two lattices suggest a description in which *the bipolaron lattice is the result of a dimerization of the polaron lattice,* as clearly illustrated in Fig. 8.

The widths of the lower and upper bipolaron bands are 0.28 eV [band *b'* in Fig. 7(a)] and 0.26 eV (band *c*), respectively, i.e., the electronic structure is almost perfectly symmetric around midgap. This feature also holds for the polaron bands, which are calculated to be 0.98 eV (band *b*) and 0.85 eV (band *c*) wide.

The first interband transition in the bipolaron lattice, between bands *b* and *b'* of Fig. 7(a), appears at 0.5 eV. It is evident from the comparison between the polaron and bipolaron lattice band structures presented in Fig. 8 that this transition has its correspondence in an intraband absorption of the half-filled polaron band. Such an absorption onsets at zero energy and can extend up to about 1.0 eV, i.e., the polaron bandwidth. These predictions for the polaron lattice are in full agreement with the experi-

mental results, which for $y \sim 0.25$ indicate an optical absorption peaking at 0.6 eV, with a long tail into the far-ir regime.[41]

For higher photon energies, we note that the bipolaron lattice would present a transition between bands b and c with an onset at 1.50 eV. It is interesting to study the evolution of this transition; for $y=0.20$, it is found at 1.47 eV, whereas for $y=0.33$, it onsets at 1.53 eV. Thus, this transition is almost independent of the doping level. A very similar behavior is observed in optical-absorption spectra of dissolved poly(3-hexylthiophene) doped up to $y=0.36$.[12] Very interestingly, no metallic properties are found in this system, suggesting that it remains in the bipolaron conformation even at very high doping levels. An absorption peaking at ~ 1.5 eV is observed for doping levels between 10% and 36%, in excellent agreement with the VEH value for the transition between the valence band and the upper bipolaron band. In contrast, for polythiophene in the solid state, which exhibits metallic properties in the highly doped state, a shift from 1.6 to 1.9 eV is observed in the doping range $y=0.14$ to $y=0.20$.[35] This shift compares much more favorably with the evolution of the transition between the polaron bands [bands b and c in Fig. 7(b)], which is located at 1.73 eV for $y=0.10$, 1.93 eV for $y=0.25$, and 2.18 eV for $y=0.33$. Furthermore, in the polaron lattice conformation there are also transitions, first between bands a and b (onsets at 1.4 eV) and also between bands a and c (onsets at 2.8 eV). These transitions explain qualitatively the finite absorption observed in the whole energy region up to ~ 2.5 eV. Finally, we observe that the π-π^* transition in the polaron lattice has its correspondence in transitions between states deep into the valence and conduction bands of the bipolaron lattice, and consequently, appears at a much higher energy than in the bipolaron lattice. The transition is calculated to onset at 2.9 eV. No sharp transition is experimentally found in the 2–3-eV region,[34,41] which is consistent with the polaron lattice model.

A schematic representation of the soliton, polaron, and bipolaron band structures is given in Fig. 8. In this figure we have, in a qualitative way, taken into account the properties of the detailed band-structure description presented previously. The closure of the Peierls gap as the system is driven from a "dimerized" bipolaron lattice conformation towards a polaron lattice conformation is clearly illustrated as well as the relation between the bandwidths and the band gaps for the respective

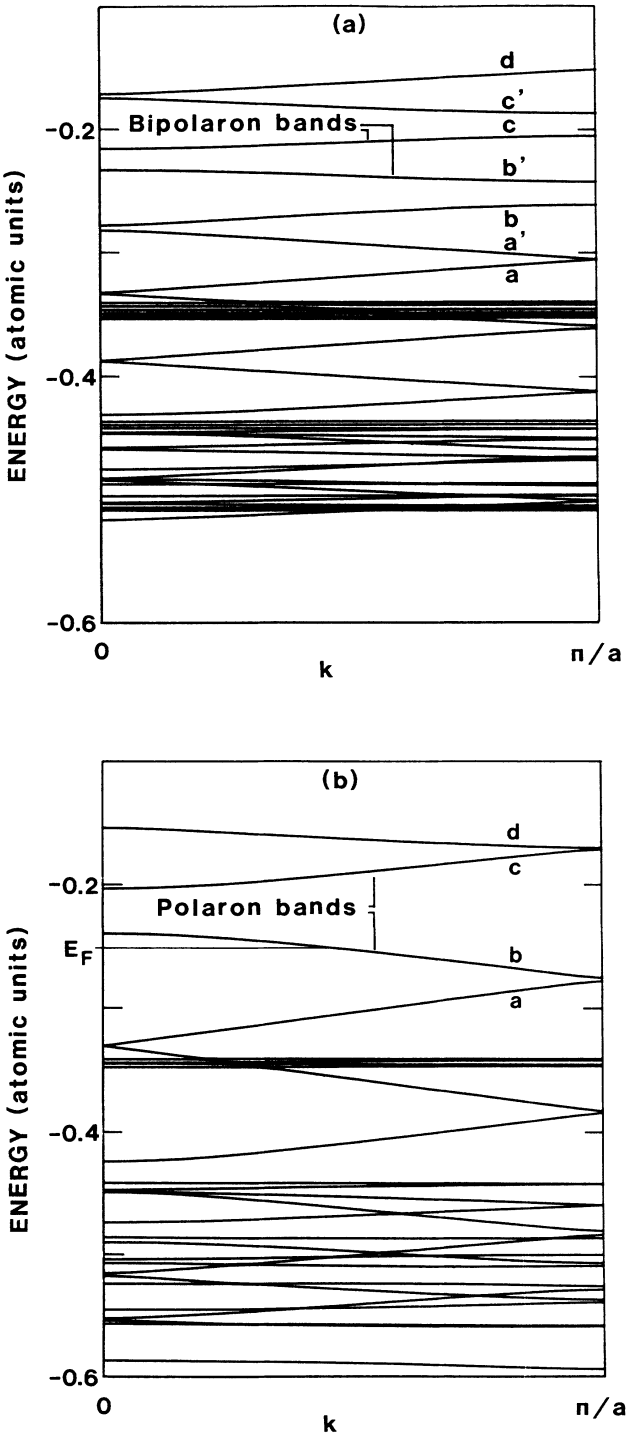

FIG. 7. VEH band structures for polythiophene at doping level $y=0.25$ for (a) the bipolaron lattice and (b) the polaron lattice.

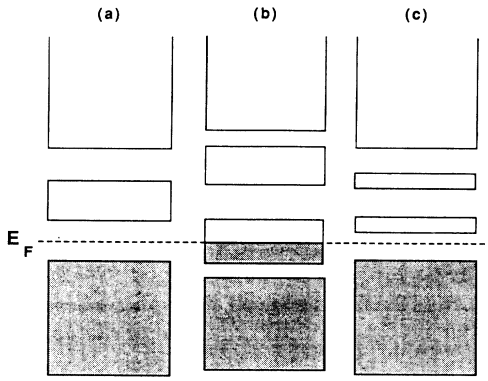

FIG. 8. Schematic representation of the band structure at high doping level for (a) the soliton lattice, (b) the polaron lattice, and (c) the bipolaron lattice.

configurations.

We stress that the polaron bands in *trans*-$(CH)_x$ and PT are both calculated to be 1.0 eV wide. Actually, by comparing the shape of the polaron bands in these two polymers [Fig. 6(b) for *trans*-polyacetylene and Fig. 7(b) for polythiophene], it is hard to notice any significant differences, the narrow subgaps between bands *a* and *b*, and bands *c* and *d* being also very similar. This similarity originates from the facts that (i) there is almost no sulfur contribution to the lower polaron band in polythiophene; (ii) the carbon backbone in polythiophene resembles that of *cis*-polyacetylene; and (iii) the charge per carbon is formally the same (0.0625) in both cases. As a result of these similarities, it is expected that, if the polaron lattice model is correct, the experimental absorption spectra of *trans*-$(CH)_x$ and PT should be very similar. This is actually the case if we compare, for example, the data given in Ref. 32 [for *trans*-$(CH)_x$] and in Refs. 35 and 41 (for PT). At high doping, both polymers exhibit an absorption tail extending into the far-ir region and a rather symmetric peak at 0.6 eV (which can be understood in terms of an intraband transition within the half-filled polaron band) as well as very broad absorptions in the 1–3 eV region.

As briefly mentioned in Sec. II, the method of using geometries optimized for oligomers as the geometry for the respective lattice configurations was questioned by Choi and Mele.[7] In particular, these authors showed that within the TLM model, the geometry of an isolated polaron is different from the geometry of a regular infinite array of polarons, i.e., the polaron lattice. Furthermore, they also found that above $y=0.06$, i.e., in the metalliclike regime, the polaron lattice is unstable with respect to an undimerized lattice conformation. This finding was used as an argument against the polaron lattice model since such a geometrical conformation cannot explain the persistence of vibrational absorption typical for localized defects at high doping levels. However, very recent MNDO calculations,[42] where the geometry of a polaron lattice up to 12% doping level is fully optimized, indicate the persistence of localized polaron defects whose geometrical characteristics are identical to those used in the calculations presented in this paper. It is our experience that optimizations on large-sized oligomers closely resemble the geometries of the corresponding polymers.[43] Therefore, if the polaron lattice model holds, we believe that the geometry presented here is a reasonable approximation to the true geometrical configuration. It must be stressed that our picture of the polaron lattice as an array of clearly distinguishable localized defects is in qualitative agreement with the observed vibrational properties of the highly doped, metalliclike polymers. A quantitative analysis would, however, be highly desirable.

VI. CONCLUSIONS

As noted in the Introduction, the sharpness of the transition into the metallic state for *trans*-polyacetylene and polythiophene is characteristic of a first-order phase transition. It is then striking that, by following the evolution of the optical properties as a function of doping, no dramatic changes do occur when the critical concentration is reached. The low-energy peak is almost unchanged and the π-π^* transition exhibits a gradual decrease in oscillator strength with doping level. The major change is the appearance of far-ir absorption which is observed in the highly doped state but not at low doping levels. It is therefore important that our band-structure calculations indicate that these small changes are consistent with the picture of a transition into a polaronic metal.

At the crossover from a soliton lattice to a polaron lattice in *trans*-polyacetylene, the *interband* transition between the valence and the soliton bands is replaced by an *intraband* transition within the half-filled polaron band. Since the polaron band fits into the energy gap between the valence band and the soliton (see Fig. 8), no major changes in the excitation properties are expected except for the onset of far-ir activity, in excellent qualitative agreement with experimental findings. In polythiophene, the similarities between the situations before and after the possible crossover from a bipolaron lattice to a polaron lattice are even more evident since the overall features of the band structure are the same for both lattice conformations [see Figs. 7(a) and 7(b)]. The main difference resides in the appearance of a finite density of states at the Fermi level when the bipolaron to polaron lattice transition takes place.

Finally, we would like to stress the following. Our band-structure calculations can only provide a qualitative picture, since at this stage we are not in a position to follow the energetics of a possible crossover from a soliton or bipolaron lattice to a polaron lattice (which could be driven by three-dimensional and/or Coulomb effects). Our approach has been to calculate the band structure for different lattice configurations and to compare the theoretical results with available experimental data. The results indicate that a description of the highly doped regime of polyacetylene and polythiophene in terms of a polaronic metal is consistent with the optical and magnetic properties at these doping levels. We stress that in contrast to the results of calculations based on simpler models, which have been used to argue against the polaron lattice model, the polaron lattice band structure we find leads to wide (~ 1 eV) polaron bands and a polaron defect that possess a marked bond alternation pattern. The next challenge will be to find quantitative results, not only with regard to the optical properties, but also as concerns the stability of the different configurations and how disorder, Coulomb, and three-dimensional effects can influence the properties of the polymers in their highly doped state.

ACKNOWLEDGMENTS

We are grateful to the Belgian National Fund for Scientific Research (FNRS), IBM-Belgium, and the Facultés Universitaires Notre-Dame de la Paix (FNDP) for the use of the Namur Computing Facility (SCF). One of us (S.S.) is supported by FNDP, the Swedish Natural Science Council, and the Swedish Board for Technical Development. Stimulating discussions with J. M. André, E. J. Mele, E. M. Conwell, and A. J. Heeger are gratefully acknowledged.

*Present address: Department of Physics, Linköping University, S-581 83 Linköping (Sweden).

†Present address; also, where correspondence concerning this paper should be sent: Service de Chimie des Matériaux Nouveaux, Université de l'Etat à Mons, B-7000 Mons (Belgium).

[1]For a review, see *Handbook of Conducting Polymers,* edited by T. A. Skotheim (Dekker, New York, 1986).

[2]S. Ikehata, J. Kaufer, T. Woerner, A. Pron. M. A. Druy, A. Sivak, A. J. Heeger, and A. G. MacDiarmid, Phys. Rev. Lett. **45**, 1123 (1980).

[3]E. J. Mele and M. J. Rice, Phys. Rev. B **23**, 5397 (1981).

[4]A. J. Epstein, in *Handbook of Conducting Polymers,* Ref. 1, p. 1041.

[5]S. Kivelson and A. J. Heeger, Phys. Rev. Lett. **55**, 308 (1985).

[6]E. Ehrenfreund, Z. Vardeny, O. Brafman, R. Weagly, and A. J. Epstein, Phys. Rev. Lett. **57**, 2081 (1987).

[7]H. Y. Choi and E. J. Mele, Phys. Rev. B **34**, 8750 (1986).

[8]K. Kume, K. Mizuno, K. Mizoguchi, K. Nomura, Y. Naniwa, J. Tanaka, M. Tanaka, and H. Watanabe, Mol. Cryst. Liq. Cryst. **83**, 285 (1982).

[9]K. Mizoguchi, K. Misuo, K. Kume, K. Kaneto, T. Shiraishi, and K. Yoshino, Synth. Met. **18**, 195 (1987).

[10]F. Moreas, D. Davidov, M. Kobayashi, T. C. Chung, J. Chen, A. J. Heeger, and F. Wudl, Synth. Met. **10**, 169 (1985).

[11]P. Pfluger, U. M. Gubler, and G. B. Street, Solid State Commun. **49**, 911 (1984).

[12]M. Nowak, S. D. D. V. Roghooputh, S. Hotta, and A. J. Heeger, Macromolecules **20**, 965 (1987).

[13]J. M. Ginder, A. F. Richter, A. G. MacDiarmid, and A. J. Epstein, Solid State Commun. **63**, 97 (1987).

[14]T. Hjertberg, W. R. Salaneck, I. Lundström, N. L. D. Somasiri, and A. G. MacDiarmid, J. Polym. Sci. Polym. Lett. Ed. **23**, 503 (1985).

[15]S. Stafström, J. L. Brédas, A. J. Epstein, H. S. Woo, D. B. Tanner, W. S. Huang, and A. G. MacDiarmid, Phys. Rev. Lett. **59**, 1464 (1987).

[16]W. P. Su, R. J. Schrieffer, and A. J. Heeger, Phys. Rev. Lett. **42**, 1698 (1979); Phys. Rev. B **22**, 2209 (1980).

[17]J. L. Brédas, B. Thémans, J. G. Fripiat, J. M. André, and R. R. Chance, Phys. Rev. B **29**, 6761 (1984).

[18]H. O. Villar and M. Dupuis, Chem. Phys. Lett. **142**, 59 (1987).

[19]M. J. S. Dewar and W. Thiel, J. Am. Chem. Soc. **99**, 4889 (1977); **99**, 4907 (1977).

[20]D. S. Boudreaux, R. R. Chance, J. L. Brédas, and R. Silbey, Phys. Rev. B **28**, 6927 (1983).

[21]G. Nicolas and Ph. Durand, J. Chem. Phys. **70**, 2020 (1979); **72**, 453 (1980).

[22]J. M. André, L. A. Burke, J. Delhalle, G. Nicolas, and Ph. Durand, Int. J. Quantum Chem. Symp. **13**, 283 (1979).

[23]J. L. Brédas, R. R. Chance, R. Silbey, G. Nicolas, and Ph. Durand, J. Chem. Phys. **75**, 255 (1981).

[24]J. L. Brédas, in *Handbook of Conducting Polymers,* Ref. 1, p. 859.

[25]H. Takayama, Y. R. Lin-Liu, and K. Maki, Phys. Rev. B **21**, 2388 (1980).

[26]C. R. Fincher, C. E. Chen, A. J. Heeger, A. G. MacDiarmid, and J. B. Hastings, Phys. Rev. Lett. **48**, 100 (1982); C. S. Yannoni and T. C. Clarke, Phys. Rev. Lett. **51**, 1191 (1983).

[27]A. Karpfen and J. Petkov, Theor. Chim. Acta. **53**, 65 (1979).

[28]A. Almenningen, O. Bastiansen, and P. Svendsas, Acta. Chem. Scand. **12**, 1671 (1958).

[29]J. L. Brédas, F. Wudl, and A. J. Heeger, Solid State Commun. **63**, 577 (1987).

[30]D. Bertho and C. Jouanin, Phys. Rev. B **35**, 626 (1987).

[31]M. J. S. Dewar, *The Molecular Orbital Theory of Organic Chemistry* (McGraw-Hill, New York, 1969), p. 185.

[32]X. Q. Yang, D. B. Tanner, M. J. Rice, H. W. Gibson, A. Feldblum, and A. J. Epstein, Solid State Commun. **61**, 335 (1987).

[33]T. C. Chung, F. Moraes, J. D. Flood, and A. J. Heeger, Phys. Rev. B **29**, 2341 (1984).

[34]S. Jeyadev and E. M. Conwell, Phys. Rev. B **33**, 2530 (1986).

[35]T. C. Chung, J. H. Kaufman, A. J. Heeger, and F. Wudl, Phys. Rev. B **30**, 702 (1984).

[36]K. Kaneto, S. Hayashi, S. Ura, and K. Yoshino, J. Phys. Soc. Jpn. **54**, 1146 (1985); K. Kaneto and K. Yoshino, Synth. Met. **18**, 133 (1987).

[37]G. Harbeke, D. Baeriswyl, H. Kiess, and W. Kobel, Phys. Scr. **T13**, 302 (1986).

[38]Z. Vardeny, E. Ehrenfreund, O. Brafman, M. Nowak, H. Schaffer, A. J. Heeger, and F. Wudl, Phys. Rev. Lett. **56**, 671 (1986).

[39]B. Horovitz, Phys. Rev. Lett. **46**, 742 (1981).

[40]J. Fink, N. Nücker, B. Scheerer, A. vom Felde, and G. Leising, in *Electronic Properties of Conjugated Polymers,* edited by H. Kuzmany, M. Mehring, and S. Roth (Springer-Verlag, Berlin, 1987), p. 84.

[41]S. Hasegawa, K. Kamiya, J. Tanaka, and M. Tanaka, Synth. Met. **18**, 225 (1987).

[42]M. C. dos Santos and J. L. Brédas (unpublished).

[43]J. M. André in *Large Finite Systems,* edited by J. Jortner, A. Pullman, and B. Pullman (Reidel, Dordrecht, 1987), p. 277.

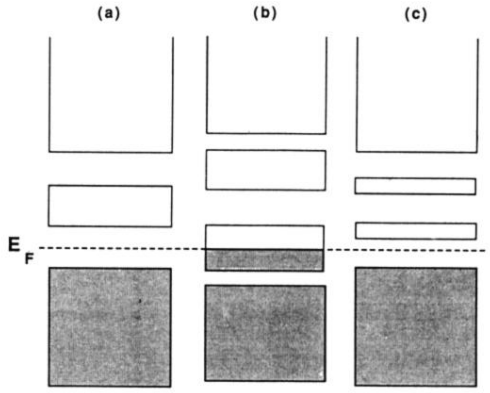

FIG. 8. Schematic representation of the band structure at high doping level for (a) the soliton lattice, (b) the polaron lattice, and (c) the bipolaron lattice.